



**SPE 164121**

## **Effective Propagation of HPAM Solutions through the Tambaredjo Reservoir during a Polymer Flood**

R.N. Manichand, SPE, K.P. Moe Soe Let, SPE, Staatsolie Suriname, L.Gil, SPE, B.Quillien, SNF SAS, and R.S. Seright, SPE, New Mexico Tech

Copyright 2013, Society of Petroleum Engineers

This paper was prepared for presentation at the SPE International Symposium on Oilfield Chemistry held in The Woodlands, Texas, USA, 8–10 April 2013.

This paper was selected for presentation by an SPE program committee following review of information contained in an abstract submitted by the author(s). Contents of the paper have not been reviewed by the Society of Petroleum Engineers and are subject to correction by the author(s). The material does not necessarily reflect any position of the Society of Petroleum Engineers, its officers, or members. Electronic reproduction, distribution, or storage of any part of this paper without the written consent of the Society of Petroleum Engineers is prohibited. Permission to reproduce in print is restricted to an abstract of not more than 300 words; illustrations may not be copied. The abstract must contain conspicuous acknowledgment of SPE copyright.

### **Abstract**

Two new methods were developed for anaerobically sampling polymer solutions from production wells in the Sarah Maria polymer flood pilot project in Suriname. Whereas previous methods indicated severe polymer degradation, the improved methods revealed that the polymer propagated intact over 300 ft through the Tambaredjo formation. This finding substantially reduces concerns about HPAM stability and propagation through low- and moderate-temperature reservoirs. Analysis of produced salinity, polymer concentration, and viscosity indicated that the polymer banks retained low salinity and therefore high viscosity for much of the way through the Sarah Maria polymer flood pilot pattern. A strong shear-thickening rheology was observed for 1000-ppm and 1350-ppm HPAM solutions in porous media, even though the salinity was only 500 ppm TDS. Examination of injectivities revealed that these solutions were injected above the formation parting pressure in the Sarah Maria polymer injection wells. Analysis suggested that the fractures extended only a short distance (~20 ft) from the injection wells and did not jeopardize sweep efficiency. In contrast, the short fractures greatly improved polymer injectivity and reduced concern about polymer mechanical degradation.

### **Introduction**

In polymer floods and other chemical floods that use water-soluble polymers for mobility control, the polymer should remain stable for most of its transit through the reservoir in order to maintain sufficient viscosity to efficiently displace oil. However, for many cases where polymer samples were collected from production wells, the polymer was severely degraded, even in low-temperature applications. Extensive sampling of production wells at Daqing revealed ~80% loss of viscosifying ability for HPAM after travelling ~800 ft through the Daqing sand at 45°C (Zhang 1995, Wang *et al.* 2008). After a residence time of 2-3 years in the Daqing reservoir, You *et al.* (2007) reported that polymer molecular weight decreased by 92% (from 19.8 million daltons to 0.89 million daltons), and the degree of hydrolysis increased by ~29% (from 28% to 36.2%). You *et al.* (2007) also reported that after transiting the Shengli reservoir (70°C, 2-3 year residence time), HPAM molecular weight decreased by 77.2% (from 17.3 million daltons to 3.94 million daltons), and the degree of hydrolysis increased by 71.5% (from 22.3% to 38.2%). After transiting the Shuanghe (Henan) reservoir (70°C, 2-4 year residence time), You *et al.* (2007) reported HPAM molecular weight decreased by 84.6% (from 15.2 million daltons to 2.35 million daltons), and the degree of hydrolysis increased by 151% (from 23.7% to 59.5%). Putz *et al.* (1994) examined HPAM produced from the Courtenay polymer flood (30°C). After transiting ~500 ft through the formation, the HPAM lost about half of its viscosifying ability. As will be described shortly, during our first testing procedures for solutions produced from the Sarah Maria polymer pilot in the Tambaredjo field (Suriname), we also observed that HPAM experienced a substantial (83%) drop in molecular weight upon transiting ~330 ft through the formation at 38°C.

The above observations are disturbing since they raise questions about when and how polymer degradation occurred. If degradation occurred during or shortly after injection, the viability of the polymer flood should be seriously jeopardized. In contrast, if degradation occurred at or near the production wells, the degradation has little/no negative impact. On a positive note, the above polymer floods exhibited very positive oil production responses. Nevertheless, since polymer costs represent a substantial part of the investment during a polymer flood, understanding where and how polymer degradation occurs can have considerable value. Previous laboratory work indicated that HPAM solutions should be quite stable at low temperatures, considering the conditions present in most low-temperature reservoirs (Shupe 1981, Yang and Treiber 1985, Moradi-Araghi and Doe 1987, Seright *et al.* 2010). So, why was severe degradation observed in the above field projects?

In this paper, we test a hypothesis that the polymer degradation occurred dominantly during the time between polymer production from the well and viscosity measurement. More specifically, our hypothesis is that when polymer solutions (even with high oxygen content) are injected into a reservoir, pyrite, siderite, and other iron minerals rapidly reduce the dissolved oxygen content to undetectable levels within a few days even at low temperatures. In this reduced condition,  $\text{Fe}^{2+}$  can readily dissolve into the polymer solution (at a level of 0.2-1.2 ppm in our specific case). This iron has no effect on the polymer so long as no free oxygen or oxidizing agent is present—so the polymer provides effective viscosity (Seright *et al.* 2010). However, once the polymer solution is produced and mixed with oxygen, the polymer can rapidly degrade.

We developed a simple sampling arrangement/procedure that allows collection of polymer samples from a well, introduction into a Brookfield viscometer, and viscosity measurement—all under anaerobic conditions. We also applied a second method, where 10 cm<sup>3</sup> of a stabilizing solution containing specific sacrificial agents and radical scavengers was mixed with the collected sample to proactively counter any iron-induced oxidative degradation that may occur when the sample is exposed to atmospheric conditions during measurements. Using these methods, we demonstrate that the HPAM polymer transported ~330 ft through the Tambaredjo reservoir with no loss of viscosifying ability. Without using these procedures, produced polymer samples lost over 75% of their viscosifying ability within an hour of collection. This paper describes the sampling procedures, and examines the effective injection and propagation of HPAM solutions in the Sarah Maria polymer flood pilot.

### The Sarah Maria Polymer Flood Pilot

**Reservoir Description.** Staatsolie's Sarah Maria polymer flooding pilot project in the Tambaredjo field (**Fig. 1**) currently has three injection wells (1M101, 1N062, and 1M052) with nine offset production wells (1M09, 1M10, 1N06, 1M051, 1N11, 1N061, 1M04, 1M05, and 1125). Solution gas drive and compaction were largely responsible for the 20% original oil in place recovery factor associated with primary recovery in the pilot area. No active water drive in this part of the field is evident, and no waterflood has been implemented. A combination of rock and fluid expansion and rock compaction appear to be responsible for most formation water produced from the project area. Average permeabilities for the T1 sand (the main productive interval) range from ~4 darcys to ~12 darcys. A significant level of heterogeneity exists in the Tambaredjo reservoir—with a 12:1 permeability contrast observed for the ~20-ft thick T1 layer and the overlying ~15-ft thick T2 layer. No significant flow barriers exist between the two layers. To supplement the compaction and solution gas drive mechanisms, polymer injection is being evaluated. High oil viscosity in the Tambaredjo field mandates that polymer injection is preferred over water injection. Produced oils range in viscosity from 1,260 to 3,057 cp, with an average of 1,728 cp. Water viscosity at reservoir temperature (100°F, 38° C) is about 0.7 cp.

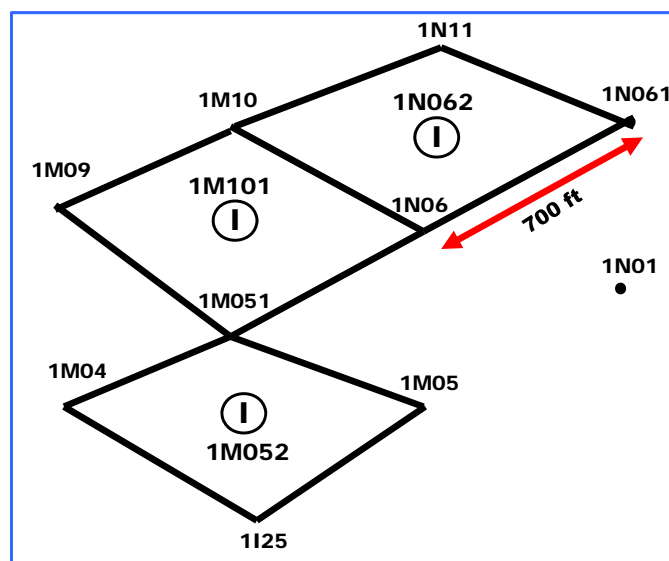


Fig. 1—Sarah Maria polymer pilot project.

**Polymer Injection and Breakthrough.** Polymer injection into Well 1M101 began in September 2008. Injection rate varied between 160 and 335 BPD (September 2008 - August 2012). As of August 2012, 335,679 bbl of polymer solution had been injected into Well 1M101. Polymer injection into Well 1N062 began in May 2010 and has continued with rates between 220 and 320 BPD. As of August 2012, 236,575 bbl of polymer solution had been injected into Well 1N062. Polymer injection in a third well, 1M052, began in June 2011. As of August 2012, 99,574 bbl had been injected at rates varying between 150 and 270 BPD. Considering the pore volume of all three injection patterns, approximately 24% PV of polymer solution had been injected as of August 2012. Oil and water cut responses to polymer injection and results from interwell tracer studies can be found in Moe Soe Let *et al.* 2012.

Polymer breakthrough was modest and gradual in the first injection pattern, being detected in the producers located west and north of the injector. In the second injection pattern, the polymer breakthrough was more evident, and higher concentrations of polymer were produced quickly in wells in the north-south direction. In the third injection pattern, polymer breakthrough also was observed in the wells south of the injector. Well 1N11 is currently producing a polymer concentration that is 66% of the 1,350-ppm injected concentration. Three wells (1N01, 1N06, and 1I25) are producing 34%-41% of the injected polymer concentration. Two wells (1M05 and 1M09) are producing 16-21% of the injected polymer concentration. Six other wells are producing small (<5%) but detectable polymer concentrations. Based on the polymer breakthrough times and concentrations, the level of channeling is significantly greater in the second injection pattern.

**Water Quality and Polymer Mixing.** The water used for mixing polymer solutions was clear, with no sign of particulates. Polymer solution concentrate was also clear and well-dissolved. Polymer preparation and water quality were uniform, reliable, and consistent, with only occasional upsets. Until November 2011, prepared polymer solutions contained 1,000-ppm SNF Flopaam 3630S HPAM (Mw~18 million daltons) in ~400-500-ppm-TDS Sarah Maria water and consistently had a viscosity ~50 cp (ambient temperature,  $7.3 \text{ s}^{-1}$ ) at the mixing facility and ~45 cp at the closest injection well (1M101). Since November 2011, the injected polymer concentration was raised to 1,350 ppm—providing a viscosity of ~85 cp (at  $7.3 \text{ s}^{-1}$ ).

At the Sarah Maria polymer project, the salinity of the injected polymer solutions is 400-500 ppm total dissolved solids (TDS), but the formation water typically has ten times higher salinity. HPAM polymers are extremely effective viscosifiers at low salinities, but they lose much of their effectiveness as salinity is raised. We expect the Sarah Maria polymer solution to lose over half its original viscosity if mixing with the formation water increased the salinity to ~4,700 ppm TDS. This type of mixing is most likely to occur if the mobility ratio is high, as at the Sarah Maria project. The mixing occurs because thin viscous fingers penetrate through the formation, so the saline formation water does not have to travel far (by diffusion or dispersion) to mix with the polymer water. As the viscosity of the polymer water is increased, this mixing effect is reduced. So, an incentive exists to inject the most viscous polymer solution that is practical. This concept was effectively demonstrated in German polymer floods where fresh-water polymer solutions were injected into formations with 17% TDS brines (Maitin 1992).

**Salinity Response.** Water in the injected polymer solutions was considerably less saline (400-500 ppm TDS) than for the formation water (2,500-5,000 ppm TDS). Thus, salinity of the produced water may reflect breakthrough from injection wells. **Fig. 2** plots salinity of the water from the pilot's production wells. The largest and most abrupt salinity drop occurred in Well 1N11—the north well in the second polymer pattern. The response started about one month after the start of polymer injection (into Well 1N062). Most of the salinity decrease occurred over a 5-month period, eventually leveling off at one-quarter of the original salinity (but still about three times the salinity of the injected water).

Relatively quick salinity responses were also seen in Wells 1N06 and 1I25. The responses in Wells 1N11 and 1N06 indicate a north-south channel through Injector 1N062. The response in Well 1I25 suggests a north-south channel through Injector 1M052. Gradual salinity declines were noted in Wells 1M09, 1M10, 1N061, and 1M05. No significant salinity change has been noted yet in Wells 1M04 and 1M051. These results indicate that the first polymer pattern shows no sign of channeling in any direction. They also suggest that channeling does not occur in the east-west direction in any of the three patterns.

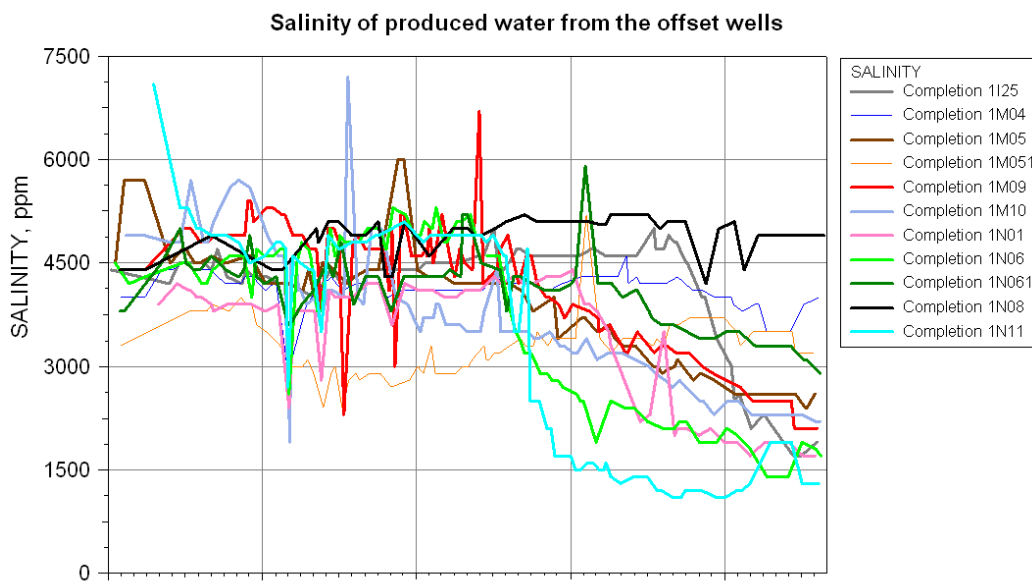


Fig. 2—Salinity responses in production wells during the polymer flood.

### First Tests of Polymer Stability

Our expectation was that the HPAM polymer should be quite stable under the conditions experienced at the Sarah Maria pilot site. The temperature was low—only 100°F (38°C) in the reservoir, so no oxidative degradation was anticipated unless a redox couple was established. However, two pieces of information caused concern. The first was that dissolved oxygen levels are ambient (3-8 ppm) throughout the mixing and injection process. The second piece of information that raised concern was from a polymer backflow test that was conducted in October-November, 2009. Although the injected polymer samples had viscosities from 40-45 cp, viscosities were noticeably less for samples back-flowed from Well 1M101. Most disturbing, an analysis indicated that the backflow samples had polymer molecular weights reduced from the original 18 million daltons to only 3 million daltons.

Three additional tests were performed in 2010, 2011, and 2012, where produced polymer samples were typically collected in a sample bomb (**Fig. 3**). These samples were shipped to France for analysis, including polymer concentration, anionicity, intrinsic viscosity, and molecular weight. **Table 1** summarizes the results from these tests. Except for those samples indicated in Table 1, all samples were collected using the sample bomb—at the time, it was presumed under anaerobic conditions. Examination of Table 1 reveals two central points. The first is that the anionicity for the produced samples were unchanged compared to the injected polymer. This result was expected since the temperature was low and pH was near neutral (Moradi-Araghi and Doe 1987). The second, and most important, point was that in all cases, the molecular weight of the produced polymer was 4-22% of the injected polymer. Further, the samples collected with the sample bomb (supposedly anaerobic) showed the same level of degradation as those collected aerobically without the sample bomb. If accepted, this result would be of major concern. Consequently, we are very interested in investigating improved sampling and measurement methods.

**Table 1—Results for samples that were shipped to France for analysis.  
Initial polymer molecular weight: 18 million daltons. Initial anionicity: ~30%.**

Sample	Polymer concentration, ppm	Anionicity, %	Intrinsic viscosity, ml/g	Molecular weight, 10 <sup>6</sup> daltons
<b>First series, 2010</b>				
1M101 Sample #OB	435	31.3	5.40	2.01
1M101 Sample #4	620	32.1	6.92	2.93
1M101 Sample #22	615	31.9	8.56	4.04
<b>Second series, 2011</b>				
1N11 with sample bomb	450	30.0	--	--
1N11 no sample bomb	454	29.4	4.31	1.43
1M09	70	26.6	3.73	1.15
1N06	244	29.4	4.40	1.48
1M05	72	23.5	3.09	0.86
1M10	15	28.5		
<b>Third series, 2012. pH values all measured between 6.5 and 6.9. Results after ultrafiltration.</b>				
1M09	140	26.2	4.79	1.68
1I25	320	31.2	7.13	3.07
1N11 with sample bomb	580	31.4	5.57	2.11
1N11 without sample bomb	550	32.4	6.02	2.37



**Fig. 3—Sample cylinder for polymer collection.**

### Improved, On-Site Sampling and Measurement Methods

We suspected that the above negative results for polymer stability occurred because oxygen was mixed with polymer solution with significant iron content, prior to measurement of polymer properties. Polymer solutions can tolerate high dissolved  $\text{Fe}^{2+}$  concentrations, so long as no free oxygen is present (Shupe 1981, Yang and Treiber 1985, Seright *et al.* 2010). If free oxygen is introduced, a redox reaction will be initiated that degrades the HPAM polymer. When the polymer solution was injected at Sarah Maria, it contained little or no dissolved iron, but it contained 3-8 ppm dissolved oxygen. However, based on literature reports and analysis (Seright *et al.* 2010) within days of injection, iron minerals in the formation remove all this dissolved oxygen. In the process,  $\text{Fe}^{2+}$  was introduced into polymer solution (0.2-1.2-ppm iron, from our measurements of produced samples). Presumably, the polymer flowed intact through the reservoir, effectively improving sweep efficiency. After arriving at the producer, introduction of free oxygen during or after sampling caused severe polymer degradation.

**First Improved Sampling Method.** To test the above concept, we collected an anaerobic sample from Well 1N11. **Fig. 3** shows the sample apparatus. During sample collection, it was very important to point the bottom end of the cylinder upward, so that gas was displaced and the cylinder was allowed to fill completely with liquid. If the cylinder was filled with the bottom end pointed downward (as occurred during previous sampling), a large pocket of air remained. Oxygen in this air could degrade the polymer. After settling overnight, to allow oil to float to the top of the cylinder, we connected the sample cylinder to a special set of fittings that allowed anaerobic liquid to flow directly from the sample cylinder into the bottom of the Brookfield viscometer's UL adapter and out the top of the UL adapter (**Figs. 4 and 5**). Just after the outlet valve of the sample cylinder, we placed a 6-inch tube section that contained a rolled paper towel to filter any oil. Although we had a nitrogen cylinder (with 300 psi nitrogen) ready to drive polymer solution from the sample cylinder into the UL adapter, it was not needed because the sample cylinder was sufficiently pressurized during collection at the wellhead.

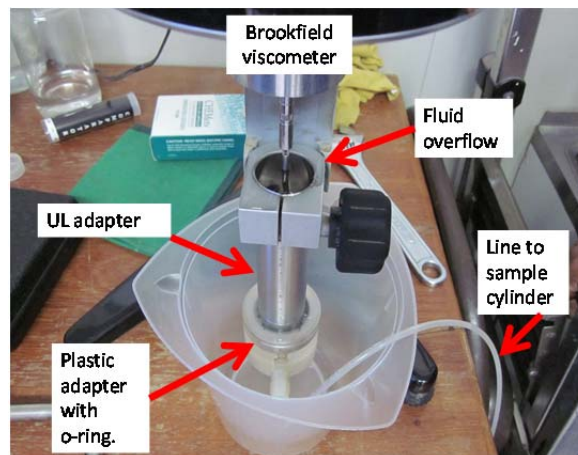


Fig. 4—Sample transfer arrangement showing connection to the viscometer.

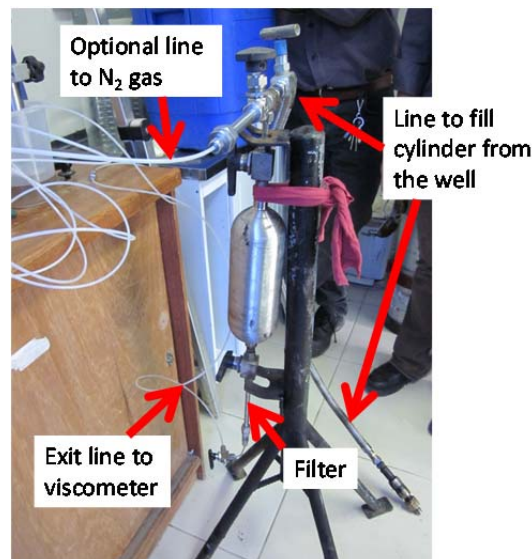


Fig. 5—Sample collection cylinder, ready to flow sample to the viscometer anaerobically.

After filling the UL adapter with polymer solution, the valve at the end (bottom) of the sample cylinder was closed and the viscometer motor was turned on—measuring viscosities from 31-34 cp, during several sampling periods. Dissolved oxygen was measured for the fluid that came out from the top of the UL adapter—revealing 10-15 ppb dissolved oxygen. Dissolved iron was measured at 0.2 ppm, and salinity was measured at 1600 ppm TDS. For comparison, an oxygenated polymer solution was collected from 1N11. Within an hour of collection, viscosity was measured at  $7.3 \text{ s}^{-1}$  (i.e., 6 rpm) and found to be 6 cp. Thus, less than one hour of contact with dissolved oxygen caused substantial viscosity loss (i.e., from 31-34 cp down to 6 cp) for the polymer solution with 0.2 ppm dissolved iron.

The polymer concentration produced from Well 1N11 contained 896 ppm HPAM. Separate measurements revealed that a freshly prepared solution of 900-ppm HPAM in 1600-ppm TDS brine should provide a viscosity of at least 20 cp (at  $7.3 \text{ s}^{-1}$ ,  $25^\circ\text{C}$ ). Our measured viscosity for the produced polymer fluid (31-34 cp) indicates that the polymer has propagated through the reservoir with no significant degradation. In support of this conclusion, we noted long, thin liquid strings at the last stage of pouring the produced polymer solutions from a container. This stringiness is caused by very high molecular weight polymers. (In contrast, polymer-free solutions show discrete drops during this procedure.) These very high molecular weight polymers are the most likely species to be destroyed or removed by (1) mechanical degradation, (2) oxidative degradation, and (3) retention within the porous media. Since these polymers were propagated  $\sim 330$  ft through the formation from Injector 1N062 to Producer 1N11, we have greater confidence that the polymer was effective in providing viscosity and effective sweep in the polymer pilot. Additional measurements were made for produced polymer samples from two other wells. The following table summarizes the results.

**Table 2—Summary of measurements of produced fluids using new sampling Method 1.**

Well	cp @ 6 rpm	Polymer ppm	TDS, ppm	Fe, ppm
1N11	31-34	896	1600	0.2
1N06	9.5	465	2390	1.0
1M051	1	0	3740	1.2

**Second Improved Sampling Method.** For the second sampling method, the configuration shown in **Fig. 6** was used. For setup and installation of this device, we first filled the  $150 \text{ cm}^3$  cylinder with  $50 \text{ cm}^3$  of stabilizing chemical solution—that contained sacrificial agents and radical scavengers. This cylinder was pressurized to 20-30 bar (290-435 psi) with nitrogen. Next, the cylinder was connected to Valve 3 via a quick coupling. After checking that all valves (in Fig. 6) were closed, the sampling system was connected to the sampling point at Valve 1.

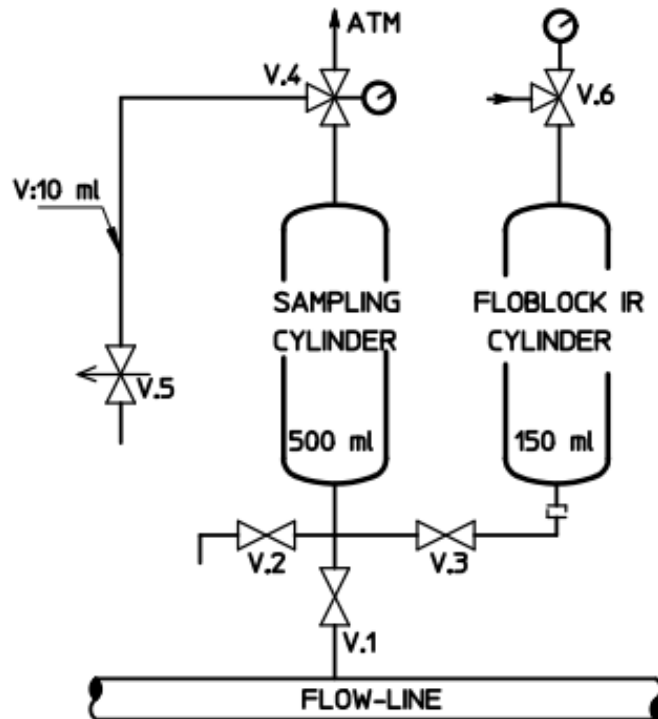


**Fig. 6—Second Improved Sampling Method.**

After installation, the sampling sequence was as follows:

- A. Collect the sample in the 500 cm<sup>3</sup> cylinder.
  1. Open Valve 1.
  2. Open the three-way Valve 4 to allow flow toward Valve 5.
  3. Open Valve 5 to waste. The flow can be regulated from this valve to avoid shear degradation. Flush the sampling cylinder with at least 1,500 cm<sup>3</sup>.
  4. Close Valve 5.
  5. Close Valve 1. If needed, release slightly the pressure in the sampling cylinder with Valve 5. The pressure should ultimately be slightly greater than atmospheric. For this particular field application, this step was not needed because the well head pressure was 3-4 bar (40-60 psi).
  
- B. Empty the capillary tube (discharge line).
  1. Open the three-way Valve 4 to the atmosphere.
  2. Open Valve 5.
  3. Drain to waste until empty.
  4. Close Valve 5.
  
- C. Add the stabilizing formulation.
  1. Open Valve 3.
  2. Open the three-way Valve 4 to waste (toward Valve 5). At this time, the addition can be sensed by touching the sampling cylinder. The capillary tube is now full of fluid, as the stabilizing chemical in pressurized cylinder is pushed in the sampling cylinder.
  3. Close Valve 3.
  4. Wait for 5 minutes.
  
- D. Fluid discharge.
  1. Open Valve 5.
  2. Open Valve 2. The fluid is flowing and can be collected in a sample bottle for measurement.

Several tests were performed to compare the two methods (see Table 3), as applied to polymer samples collected from production wells 1N11 and 1N06. The highest viscosity values (measured at 7.3 s<sup>-1</sup>, room temperature) were recorded using Method 1, which did not add a chemical stabilizer and which transferred the produced solution anaerobically from the sample collection cylinder into the Brookfield viscometer. Samples collected using Method 2, but without adding stabilizer, provided higher viscosities (15 cp for 1N11 and 9 cp for 1N06) than from direct aerobic sample collection (6 cp for 1N11). Samples collected using Method 2, with a single 10 cm<sup>3</sup> dose of stabilizer, provided even higher viscosities (19.5 cp for 1N11 and 9.5 cp for 1N06). Samples collected using Method 2, with a triple dose of stabilizer, provided viscosities that approached those for Method 1.

**Table 3—Comparison of measurements of produced fluids using Methods 1 and 2.**

Well	1N11	1N06
Polymer, ppm	896	465
	cp@ 7.3 s <sup>-1</sup>	
Direct aerobic sampling	6	5
Method 1 (no stabilizer)	32	14
Method 2, no stabilizer	15	9
Method 2, single dose of stabilizer	19.5	9.5
Method 2, triple dose of stabilizer	30	12

Method 1 consistently provided the highest viscosities—suggesting the least polymer degradation during collection and measurement. However, this method requires a sample cylinder (Fig. 3), typically for a 24-hour period while gravity separates oil from the water. If multiple samples are to be collected at the same time, multiple sample cylinders are needed. In contrast, Method 2 allows several samples to be collected in a short time with a single sample cylinder.

Several improvements are being incorporated into Method 2, including: (1) A pressure gauge can be installed on the cylinder containing the stabilizing chemical. Indeed, residual pressure in the cylinder aids proper chemical addition. (2) Higher chemical addition resulted in higher viscosities. A stabilizing chemical with higher/lower dosage can be formulated so that a single dosage can be applied for a given sample. (3) Also, to avoid capillary pipe blockage (which is detrimental to chemical addition), one pipe can be installed for flushing purposes and another pipe for chemical addition with larger diameter and shorter length to allow easier clean-out of oil before each sampling.

### Oxygen in the Injection Water

Ambient levels (3-8 ppm) of dissolved oxygen were present in the Sarah Maria polymer source water and in the injected polymer solutions. Fortunately, pyrite ( $\text{FeS}_2$ ) and siderite ( $\text{FeCO}_3$ ) are commonly present in reservoirs and can quickly consume any dissolved oxygen. Using a geochemical simulator, Seright *et al.* (2010) demonstrated that a reservoir at 25°C with 1% pyrite would reduce a solution that originally contained 5,000 ppb (parts per billion) dissolved oxygen to less than 1 ppb  $\text{O}_2$  in less than four days. They also performed experiments with an HPAM solution with 3,300-ppm  $\text{O}_2$  that was placed in contact with anaerobic sand from the Daqing reservoir (containing 0.23% pyrite and 0.51% siderite). Within 24 hours at 45°C, the dissolved oxygen level was reduced from 3,300 ppb to 0 ppb, with less than 7% loss of solution viscosity. Since cores from the Sarah Maria pilot project contained up to 12% pyrite/siderite, we also expect dissolved oxygen to be removed quickly from the injected fluids. Dissolved oxygen measurements from produced water at the Sarah Maria pilot were very low (e.g., less than 20 ppb). However, because of oil interference with the colorimetric detection method, we could not definitively state that the produced dissolved oxygen content was zero.

### Dilution of Sarah Maria HPAM Solutions by Tambaredjo Brine

At the Sarah Maria polymer pilot, low-salinity Sarah Maria water is used to dissolve the HPAM. After this polymer solution is injected, it will mix to some degree with the resident Tambaredjo brine, which has a salinity 9-10 times higher than the Sarah Maria source water (4700 versus 500 ppm total dissolved solids, TDS). For a given concentration, HPAM polymers are known to provide much lower viscosities as salinity increases. This fact raises concern about (1) how much viscosity loss will occur, as a function of the degree of mixing of Sarah Maria polymer solutions with Tambaredjo brine and (2) how much in situ mixing occurs during the Sarah Maria polymer flood.

**How Much Viscosity Loss Will Occur, as a Function of the Degree of Mixing?** Based on a field water analysis, we prepared a synthetic version of the Sarah Maria source water that contains 200-ppm  $\text{MgSO}_4$ , 120-ppm  $\text{Na}_2\text{SO}_4$ , 100-ppm  $\text{NaCl}$ , and 80-ppm  $\text{CaCl}_2$ . We also prepared a synthetic version of the Tambaredjo brine with 3950-ppm  $\text{NaCl}$ , 400-ppm  $\text{MgCl}_2$ , and 350-ppm  $\text{CaCl}_2$ . Both brines were filtered through 0.45  $\mu\text{m}$  filters before polymer addition. For each brine, polymer solutions were prepared using HPAM concentrations from 200 to 5000 ppm. The 3630S HPAM was taken from the Sarah Maria pilot site (July 2012). For each solution, viscosity measurements were made as a function of shear rate at 25°C using an Anton Paar MCR301 rheometer.

**Fig. 7** plots viscosity (at 7.3  $\text{s}^{-1}$ , 25°C) versus polymer concentration in Sarah Maria source water (solid circles) and in Tambaredjo brine (open diamonds). For polymer concentrations above 1000 ppm, the relation between viscosity ( $\mu$ , in cp) and concentration ( $C$ , in ppm) is described well by Eq. 1 in Sarah Maria source water and by Eq. 2 in Tambaredjo brine. **Table 4** reveals that for much of the concentration range, for a given polymer concentration, the viscosity (at 7.3  $\text{s}^{-1}$ ) was about 3.6 times higher in Sarah Maria water than in Tambaredjo brine.

$$\mu = 10^{-4} C^{1.8575} \dots\dots\dots(1)$$

$$\mu = 10^{-5} C^{1.9671} \dots\dots\dots(2)$$

**Table 4—Comparison of Viscosities (7.3  $\text{s}^{-1}$ , 25°C) in Sarah Maria vs Tambaredjo waters.**

Polymer concentration, ppm	Viscosity in Sarah Maria water, cp	Viscosity in Tambaredjo brine, cp	Viscosity ratio
5000	714	223	3.2
3000	288	78.2	3.7
2000	131	35.3	3.7
1500	74.9	20.4	3.7
1200	49.4	13.6	3.6
1000	35.7	10.1	3.5
700	19.8	6.0	3.3
500	12.2	3.9	3.1
300	6.0	2.4	2.5
200	3.8	1.8	2.1

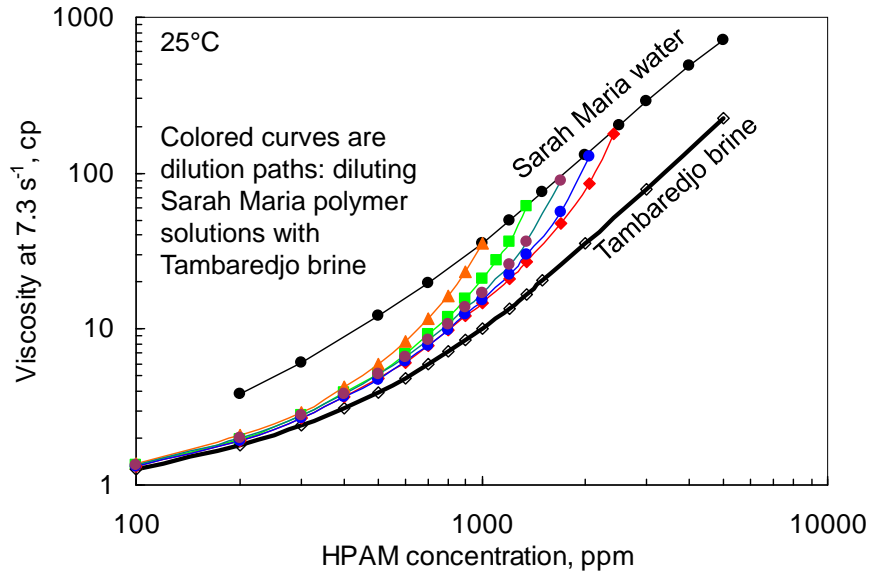


Fig. 7—Viscosity vs. concentration at 7.3 s<sup>-1</sup>, 25°C.

For five polymer solutions in Sarah Maria water—1000-ppm, 1350-ppm, 1700-ppm, 2050-ppm, and 2400-ppm HPAM, we made dilutions with Tambaredjo brine and measured viscosities (Fig. 7). The dilution path for 1000-ppm HPAM is described well (correlation coefficient: 0.9991) using Eq. 3, while the dilution path for 1350-ppm HPAM is described well (correlation coefficient: 0.9978) using Eq. 4. The dilution path for 1700-ppm HPAM is described well (correlation coefficient: 0.9928) using Eq. 5, although the fit prediction is 16% too high at 100-ppm polymer. The dilution path for 2050-ppm HPAM is described moderately well (correlation coefficient: 0.9882) using Eq. 6, although the fit prediction is 24% too high at 100-ppm polymer and a few percent low for concentrations between 400 and 1200 ppm. The dilution path for 2400-ppm HPAM is described (correlation coefficient: 0.9831) using Eq. 7; the fit prediction is 36% too high at 100-ppm polymer, and typically 10% low for concentrations between 500 and 1000 ppm.

$$\mu = 1.0151 e^{0.0035C} \dots\dots\dots(3)$$

$$\mu = 1.1243 e^{0.0029C} \dots\dots\dots(4)$$

$$\mu = 1.3035 e^{0.0025C} \dots\dots\dots(5)$$

$$\mu = 1.4216 e^{0.0023C} \dots\dots\dots(6)$$

$$\mu = 1.6045 e^{0.0020C} \dots\dots\dots(7)$$

**Table 5** compares viscosities at various points along the dilution paths. **Table 6** provides the resultant salinities upon mixing for the solutions described in Table 5.

Table 5—Viscosities (cp at 7.3 s<sup>-1</sup>, 25°C) at various points along the dilution paths.

HPAM concentration, ppm	Viscosity in Sarah Maria water, cp	Viscosity, cp, along dilution path, starting at given HPAM concentration					Viscosity in Tambaredjo brine, cp
		1000 ppm	1350 ppm	1700 ppm	2050 ppm	2400 ppm	
2400	177					177	44.6
2050	127				127	84.9	32.7
1700	89.5			89.5	56.6	47.8	22.6
1350	61.1		61.1	36.2	29.8	27.2	16.5
1000	35.7	35.7	21.0	17.0	15.4	14.6	10.1
700	19.8	11.6	9.2	8.5	7.8	7.8	6.0
500	12.2	6.0	5.2	5.1	4.8	4.8	3.9
300	6.0	2.9	2.8	2.8	2.7	2.6	2.4
200	3.8	2.1	2.0	2.0	1.9	1.9	1.8

**Table 6—Salinities (ppm TDS) at various points along the dilution paths for Table 5.**

HPAM concentration, ppm	Sarah Maria salinity, ppm TDS	Salinity, ppm TDS, along dilution path, starting at given HPAM concentration					Tambaredjo salinity, ppm TDS
		1000 ppm	1350 ppm	1700 ppm	2050 ppm	2400 ppm	
2400	500					500	4700
2050	500				500	1113	4700
1700	500			500	1217	1725	4700
1350	500		500	1365	1934	2338	4700
1000	500	500	1589	2229	2651	2950	4700
700	500	1760	2522	2971	3266	3475	4700
500	500	2600	3144	3465	3676	3825	4700
300	500	3440	3767	3959	4085	4175	4700
200	500	3860	4078	4206	4290	4350	4700

**How Much In Situ Mixing Occurs during the Sarah Maria Polymer Flood?** An important principle of polymer flooding is that a very efficient (piston-like) displacement of a reservoir can occur if the injected polymer viscosity is as large as the product of waterflood mobility ratio times the permeability contrast (Wang *et al.* 2008, Seright 2010). For that case, minimum mixing should occur between the injected polymer solution and the displaced water. At Sarah Maria, given an endpoint mobility ratio of 0.07, an oil viscosity of 600 cp, and a permeability contrast of 10:1, the optimum injected viscosity could be 420 cp. For injected viscosities less than this value, some level of mixing should be expected for the polymer solution and the formation water.

**What Factors Promote In Situ Mixing and Salinity Increase?** At least three factors promote mixing of aqueous fluids in the formation and increased salinity for the polymer bank—crossflow, ion exchange, and diffusion/dispersion. We note that the water cut for the pilot averaged about 50%, well before water or polymer injection began. Since no active water drive was present at this time, the consensus is that mobile water was present since discovery of the field. Accepted reservoir engineering (Craig 1971) indicates that mobile and connate water should be displaced efficiently, without much mixing if that water exists in the most-permeable pathway. However, if crossflow can occur, polymer solution that crossflows into the less-permeable zones can have a large area of contact with saline water in the less-permeable zones, and therefore mixing could occur.

Ion exchange from formation clays can also increase salinity of low-salinity polymer solutions. While in contact with the resident formation brine, existing clays may be heavily loaded with ions, especially calcium and magnesium. Those ions will be released into the low-salinity polymer bank when it passes (Lake 1989).

Diffusion/dispersion is a third factor that promotes mixing and salinity increase in the polymer bank. The dispersion process is associated with convective mixing during flow, and the crossflow phenomenon mentioned above is a part of this process. The dispersivity ( $\alpha$ ) in reservoirs has been suggested to be (roughly) proportional to the distance travelled by the injected bank (Arya *et al.* 1988). Diffusion is a relatively slow process that is proportional to the square root of time of contact between the polymer bank and the displaced brine bank (Lake 1989, Seright 1991a).

**How Much Did the Salinity of the Polymer Bank Actually Increase?** Fig. 2 indicates produced water salinities (during polymer flooding) that dropped to 1100-ppm TDS in Well 1N11 and to 2000-ppm TDS in Wells 1N06 and 1N01. In February 2012, analysis revealed HPAM concentrations of ~700 ppm in Well 1N11, ~350 ppm in Well 1N06, and ~380 ppm in Well 1N01. Assume that the polymer concentration reflects the contribution of the production that comes from a polymer injector (injecting 1000-ppm HPAM). So in Well 1N11, the polymer was diluted from 1000 ppm to 700 ppm. If the injected water had 500-ppm TDS salinity, an equivalent dilution with 4700-ppm TDS Tambaredjo brine should result in a produced salinity of 1800-ppm TDS. Instead, a salinity of ~1100 ppm-TDS was observed.

For Wells 1N06 and 1N01, the polymer was diluted from 1000 ppm to ~350 ppm. If the injected water had 500-ppm TDS salinity, an equivalent dilution with 4700-ppm TDS Tambaredjo brine should result in a produced salinity of 3230-ppm TDS. Instead, a salinity of ~2000-ppm TDS was observed. Since the observed salinity of the produce water was less than expected, this suggests that the in situ mixing mechanisms mentioned above (crossflow, ion exchange, dispersion/diffusion) were not as active as we might have feared. It suggests that the polymer banks may retain low salinity and therefore high viscosity for much of the way through the pattern.

### Rheology in Porous Media, Mechanical Degradation, and Injectivity

**Rheology and Mechanical Degradation.** In this section, we consider whether the polymer was expected to experience mechanical degradation during injection. Results from this analysis impact our conclusions about injectivity and the presence of near-wellbore fractures in the injection wells. Rheology in porous media and mechanical degradation are directly related to the fluid velocity or flux in porous media (Maerker 1975, Seright *et al.* 2009, Seright *et al.* 2011). Consequently, using the methods described in Seright *et al.* 2011, we determined rheology in a 4-darcy porous medium for the two polymer concentrations that have been used at the Sarah Maria pilot: (1) 1000-ppm HPAM in Sarah Maria water (500-ppm TDS) and

(2) 1350-ppm HPAM in Sarah Maria water. Figure 8 plots resistance factor versus flux for these solutions. (Resistance factor is the effective viscosity in porous media, relative to water. See Jennings *et al.* 1971 or Seright *et al.* 2011.) Fig. 9 plots viscosity (measured at  $7.3 \text{ s}^{-1}$ ,  $25^\circ\text{C}$  and expressed as a percentage of the injected polymer solution viscosity) for the effluent versus flux at which the polymer solution was forced through the core.

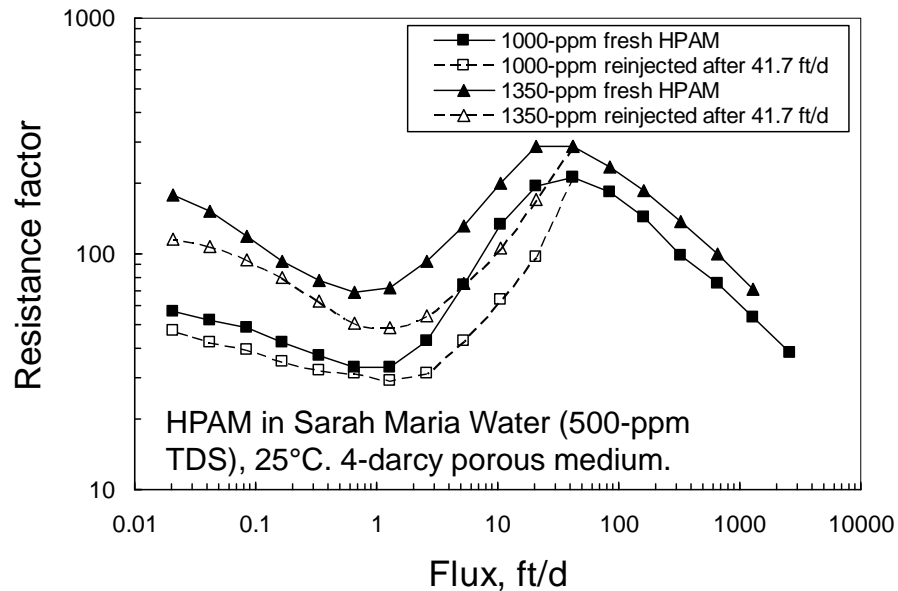


Fig. 8—Resistance factor versus flux for HPAM in Sarah Maria water.

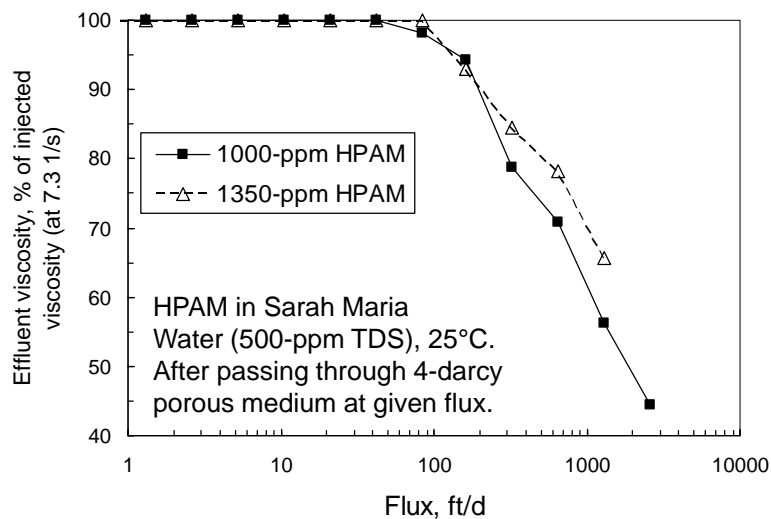


Fig. 9—Viscosities of solutions after being forced through the core at a given flux.

Fig. 8 was generated as follows. First, the core was saturated with Sarah Maria water, and porosity and permeability were determined. Next, we injected freshly prepared 1000-ppm 3630S (in Sarah Maria water) at high flux (2609 ft/d) and measured the stabilized resistance factor in the second section of the core (the core had one internal pressure tap, to eliminate end effects associated with the inlet face. See Seright *et al.* 2009). Then we halved the injection rate and allowed pressures to stabilize and resistance factor to be determined again. This process was repeated in stages to determine the resistance factors associated with the solid squares in Fig. 8. Between 2609 and 41.7 ft/d, the resistance factor appeared to increase with decreasing flux. However, this behavior was not shear thinning. For each flux between 41.7 and 2609 ft/d, the polymer was mechanically degraded to a different extent, as demonstrated by the solid squares in Fig. 9.

As flux was lowered from 41.7 ft/d to 1 ft/d, resistance factor decreased dramatically with decreasing flux (Fig. 8) and little or no mechanical degradation occurred (Fig. 9). For fluxes lower than 1 ft/d, shear thinning was seen as resistance factor increased with decreasing flux. If the salinity had been higher (than 500-ppm TDS), Newtonian or near Newtonian behavior would have been seen in this flux range, depending on polymer concentration and molecular weight (Seright *et al.* 2009,

Seright *et al.* 2011). This behavior has been consistently reported by experimentalists in the literature for the past 40 years (Jennings *et al.* 1971, Maerker 1975, Heemskerk *et al.* 1984, Seright 1991b, Seright *et al.* 2011). Oddly, a misconception persists that HPAM solutions show only Newtonian or shear-thinning behavior in porous media—not shear thickening (Lake 1989).

Next, we forced fresh 1000-ppm 3630S through the core at 41.7 ft/d and collected the effluent. This flux (~40 ft/d) is the condition that the polymer would have experienced at the Sarah Maria pilot if the completion was openhole, 8-inches in diameter, 300 BPD, 10-ft formation height (and no fracture was present). The effluent from this experiment was re-injected using a series of lower rates to obtain the open squares in Fig. 8. Note that only shear-thickening behavior is seen between 41.7 ft/d and 1 ft/d. Below 1 ft/d, some shear thinning is seen.

Next, we repeated the above steps with 1350-ppm 3630S to obtain the solid triangles (for fresh HPAM) and the open triangles (for polymer that had previously experienced 41.7 ft/d, as at the injection face for an openhole completion) in Fig. 8. A key conclusion from Fig. 9 was that mechanical degradation was expected to be small (for the actual injection condition of 300 BPD)—even if the completion was openhole (and sandface flux was ~40 ft/d). As will be demonstrated next, the injection wells actually have open fractures during polymer injection—thus creating a much greater area to flow and minimizing mechanical degradation.

**Injectivity.** The open squares and open triangles in Fig. 8 are the relevant curves if we want to estimate injectivity for these solutions. These curves were input (along with field injection conditions) to calculate injectivity (relative to water) for unfractured vertical wells with radial flow. (The method is described in Seright *et al.* 2009.) Fig. 10 shows the injectivity predictions as a function of polymer penetration away from the well. This figure clearly shows that if flow is radial for vertical openhole injection wells (with no fractures), injectivity should be dramatically less for polymer solutions than for water. Specifically, polymer solution injectivity should be only 1-2% of that for water.

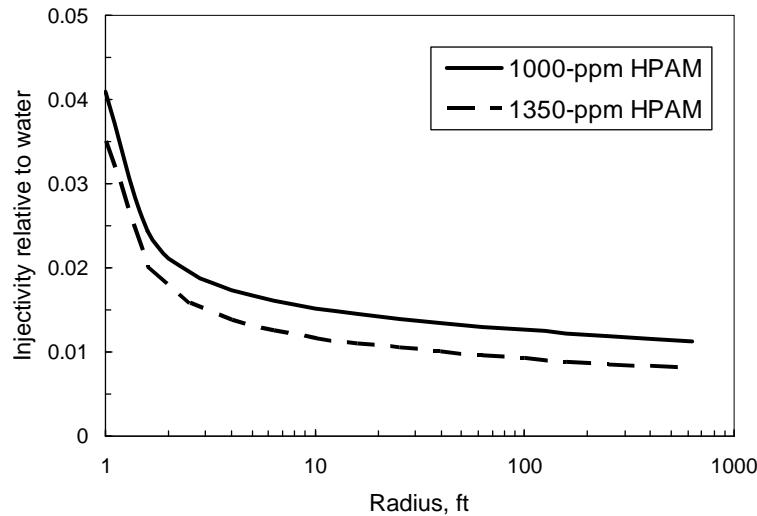


Fig. 10—Injectivity predictions assuming unfractured openhole vertical Sarah Maria injectors.

The results in Fig. 10 can be appreciated on a simpler level by realizing that resistance factors for the dashed curves in Fig. 8 never fall below (1) 29 for 1000-ppm HPAM and (2) 49 for 1350-ppm HPAM. If flow is truly radial away from the injector (as in an openhole completion with no fracture, injectivity (relative to water) for a Newtonian fluid can be estimated by Eq. 8:

$$I/I_o = \ln(r_e/r_w) / [F_r \ln(r_p/r_w) + \ln(r_e/r_p)] \dots\dots\dots(8)$$

In this equation,  $r_p$  is the radius of the polymer front,  $F_r$  is the resistance factor (minimum of 29 and 49 in our cases),  $r_e$  is external drainage radius, and  $r_w$  is wellbore radius. A few calculations with this equation reveals that for even small polymer-front radii, the injectivity is predicted to rapidly fall to less than 4% of the water injectivity (i.e., 1/29) for the 1000-ppm polymer and to 2% (i.e., 1/49) for the 1350-ppm polymer. The actual injectivity losses will be greater because the actual resistance factors will be greater (than 29 or 49) for the vast majority of the flow field.

How do the predictions from Fig. 10 compare with the observed injectivity behavior in the Sarah Maria polymer flood pilot? Consider Injection Well 1M101 in August 2008. As shown in **Table 7**, water was injected first at a low rate (100 BPD), resulting in a downhole pressure of 553 psi and an injectivity of 0.28 BPD/psi. When the rate was raised to 650 BPD, the injectivity more than tripled to 1.01 BPD/psi —indicating that a fracture was open at the high rate. When the water rate was dropped to 125 BPD, the injectivity dropped to 0.44 BPD/psi—suggesting that the fracture closed substantially. When

the rate was raised again to 650 BPD, injectivity tripled to 1.21 BPD/psi—indicating a re-opening of the fracture. Dropping the water rate again to 175 BPD dropped injectivity to 0.65 BPD/psi—indicating at least partial fracture closure. When water rate was raised a third time to 650 BPD, injectivity rose to 1.48 BPD/psi—indicating fracture re-opening. Thus, the process of opening and closing the fracture was at least partially reversible. Since this was the first time that water had been injected into this well, it seems likely that injectivity should increase with increased water injection volume—because low-viscosity water displaced some viscous oil away from the wellbore. Also, note that for this last water injection step, the downhole pressure was 638 psi—well below the accepted formation parting pressure of 800 psi—and yet the fracture was obviously open.

**Table 7—Injectivity Test of August, 2008, in Well 1M101**

Injectant	Injection rate BPD	BHP psi	Injectivity BPD/psi
water	100	553	0.28
water	650	845	1.01
water	125	482	0.44
water	650	737	1.21
water	175	471	0.65
water	650	638	1.48
1000-ppm polymer	175	635	0.40

Finally, in Table 7, note that 1000-ppm polymer solution was injected at 175 BPD, resulting in a downhole pressure of 635 psi and an injectivity of 0.40 BPD/psi. Let's assume that the fracture was closed during the previous water injection at 175 BPD, where injectivity was 0.65 BPD/psi. If no fractures are open, the expected injectivity during injection of 1000-ppm HPAM (from Fig. 10) would be reduced to ~1% of that of water or ~0.0065 BPD/psi. Instead, the observed injectivity was 0.40 BPD/psi or ~ 61 times higher than expected! Thus, a fracture was open during polymer injection.

A similar observation was found for the second injector, Well 1N062, in May 2010. Water was injected first at 343 BPD, resulting in a downhole pressure of 488 psi and an injectivity of 1.19 BPD/psi. When the rate was raised to 685 BPD, the downhole pressure increased to 638 psi and injectivity increased to 1.56 BPD/psi. This 31% injectivity increase might indicate fracture opening, but the point is debatable. However, when 1000-ppm polymer solution was injected at 343 BPD, the downhole pressure was 744 psi and injectivity was 0.63 BPD/psi. If no fractures were open, the expected injectivity for polymer solution should have been ~0.012 BPD/psi. The actual polymer injectivity was ~52 times greater than expected. So again, the fracture was open during polymer injection.

Previous work (Gadde and Sharma 2001, Seright *et al.* 2009) indicates that once fractures are opened, the fracture area increases to accommodate increased injection rate or increased injectant viscosity—with small increases in downhole pressure. This concept can be used to make a rough estimate of the open fracture area and the extent of the fracture. For example, if the injectivity is 61 times greater than expected for injection into an openhole completion, the fracture area is roughly 61 times greater than that associated with the open hole. Since the openhole area is about 42 ft<sup>2</sup> for our wells, the implied area during polymer injection is 2562 ft<sup>2</sup>. Given the depth of the Tambaredgo formation (1000 ft) and the local stress field, induced fractures are horizontal. Thus, a fracture area of 2562 ft<sup>2</sup> translates to a horizontal fracture (with an upper and lower face) that extends 20 ft from the well. This short fracture does not jeopardize sweep (i.e., create severe channeling) since the nearest production well is over 300 ft away. This point is consistent with our observation that severe channeling did not occur during the Sarah Maria polymer pilot (Moe Soe Let *et al.* 2012). However, the fracture tremendously increases injectivity for the polymer solution. The fracture also reduced the possibility of HPAM mechanical degradation. By increasing the sandface area by a factor of 61, the velocity when the polymer enters the formation is reduced in proportion.

## Conclusions

1. Two new methods were developed for anaerobically sampling polymer solutions from production wells in the Sarah Maria polymer flood pilot project in Suriname. Whereas previous methods indicated severe polymer degradation, the improved methods revealed that the polymer propagated intact over 300 ft through the Tambaredjo formation. This finding substantially reduces concerns about HPAM stability and propagation through low- and moderate-temperature reservoirs.
2. Analysis of produced salinity, polymer concentration, and viscosity indicated that the polymer banks retained low salinity and therefore high viscosity for much of the way through the Sarah Maria polymer flood pilot pattern.
3. A strong shear-thickening rheology was observed for 1000-ppm and 1350-ppm HPAM solutions in porous media, even though the salinity was only 500-ppm TDS. Injectivity analysis revealed that these solutions were injected above the formation parting pressure in the Sarah Maria polymer injection wells.
4. Analysis suggested that the fractures extended only a short distance (~20 ft) from the injection wells and did not jeopardize sweep efficiency. In contrast, the short fractures greatly improved polymer injectivity and reduced concern about polymer mechanical degradation.

## Nomenclature

- $C$  = polymer concentration, parts per million (ppm) [mg/L]  
 $F_r$  = polymer solution resistance factor (brine mobility divided polymer solution mobility)  
 $I/I_o$  = injectivity relative to water  
 $PV$  = pore volumes of fluid injected  
 $r_e$  = external drainage radius, ft [m]  
 $r_p$  = radius of polymer penetration, ft [m]  
 $r_w$  = wellbore radius, ft [m]  
 $\alpha$  = dispersivity, ft [m]  
 $\mu$  = viscosity, cp [mPa-s]

## References

- Arya, A. and Lake, L. 1988. Dispersion and Reservoir Heterogeneity. *SPE Reservoir Engineering* (Feb. 1988) 139-48.
- Craig, F.F. 1971. *The Reservoir Engineering Aspects of Waterflooding*. Monograph Series, SPE, Richardson, Texas **3**: 45-75.
- Gadde, P.B. and Sharma, M.M. 2001. Growing Injection Well Fractures and Their Impact on Waterflood Performance. Paper SPE 71614 presented at the SPE Annual Technical Conference and Exhibition, New Orleans, Louisiana, 30 September-3 October.
- Heemskerk, J., Rosmalen, R.J., Hotslag, R.J., and Teeuw, D. 1984. Quantification of Viscoelastic Effects of Polyacrylamide Solutions. Paper SPE 12652 presented at the SPE/DOE Symposium on Enhanced Oil Recovery Symposium, Tulsa, Oklahoma, 15-18 April.
- Jennings, R.R., Rogers, J.H., and West, T.J. 1971. Factors Influencing Mobility Control by Polymer Solutions. *J Pet Technol* **23** (3): 391-401; *Trans., AIME*, **251**. SPE-2867-PA. doi: 10.2118/2867-PA.
- Lake, L.W. 1989. *Enhanced Oil Recovery*, 323-324, 396-400. Englewood Cliffs, New Jersey: Prentice Hall.
- Maerker, J.M. 1975. Shear Degradation of Partially Hydrolyzed Polyacrylamide Solutions. *SPE J.* **15** (4): 311-322; *Trans., AIME*, **259**. SPE-5101-PA. doi: 10.2118/5101-PA.
- Maitin, B.K. 1992. Performance Analysis of Several Polyacrylamide Floods in North German Oil Fields. Paper SPE 24118 presented at the SPE/DOE Symposium on Improved Oil Recovery, Tulsa, Oklahoma, 22-24 April.
- Manichand, R.N., Mogollon, J.L., Bergwijn, S., Graanooogst, F., Ramdaja, R. 2010. Preliminary Assessment of Tambaredjo Heavy Oilfield Polymer Flooding Pilot Test. Paper SPE 138728. Presented at the Latin American and Caribbean Petroleum Engineering Conference. Lima, Peru. 1-3 December.
- Moe Soe Let, K.P., Manichand, R.N., and R.S. Seright. 2012. Polymer Flooding a ~500-cp Oil. Paper SPE 154567 presented at the Eighteenth SPE Improved Oil Recovery Symposium. Tulsa, Oklahoma, USA, 14-18 April 2012.
- Moradi-Araghi, A. and Doe, P.H. 1987. Hydrolysis and Precipitation of Polyacrylamide in Hard Brines at Elevated Temperatures. *SPE Reservoir Engineering* **2**(2): 189-198.
- Putz, A.G., Bazin, B., and Pedron, B.M. 1994. Commercial Polymer Injection in the Courtenay Field, 1994 Update. Paper SPE 28601 presented at the 1994 Annual Technical Conference and Exhibition. New Orleans, LA. 25-28 September.
- Seright, R.S. 1991a. Impact of Dispersion on Gel Placement for Profile Control. *SPE Reservoir Engineering* (Aug. 1991) 343-352.
- Seright, R.S. 1991b. Effect of Rheology on Gel Placement. *SPE Res Eng* **6** (2): 212-218; *Trans., AIME*, **291**. SPE-18502-PA. doi: 10.2118/18502-PA.
- Seright, R.S., Seheult, J.M., and Talashek, T.A. 2009. Injectivity Characteristics of EOR Polymers. *SPE Reservoir Evaluation and Engineering* **12** (5): 783-792.
- Seright, R.S., Campbell, A.R., Mozley, P.S., and Han, P. 2010. Stability of Partially Hydrolyzed Polyacrylamides at Elevated Temperatures in the Absence of Divalent Cations. *SPE Journal* (June 2010) 341-348.
- Seright, R.S. 2010. Potential for Polymer Flooding Viscous Oils. *SPE Reservoir Evaluation and Engineering* **13**(6): 730-740.
- Seright, R.S., Fan, T., Wavrik, K., and Balaban, R.C. 2011. New Insights into Polymer Rheology in Porous Media. *SPE Journal* (March) 35-42. SPE 129200.
- Shao, Z.B., Zhou, J.S., Sung, G., Niu, J.G., Liu, F.Q., Han, Z.R. 2005. Studies on Mechanical Degradation of Partially Hydrolyzed Polyacrylamide in Course of Polymer Flooding: Changes in Relative Molecular Mass, Viscosity and Related Parameters. *Oilfield Chemistry*. **22**(1). 25 March 2005. 72-77.
- Shupe, R.D. 1981. Chemical Stability of Polyacrylamide Polymers. *J Pet Technol* **33**(8): 1513-1529.
- Wang, Dongmei, Han, Peihui, Shao, Zhenbo, Weihong, Hou, and Seright, R.S. 2008. Sweep Improvement Options for the Daqing Oil Field. *SPE Reservoir Evaluation and Engineering* (February 2008) 18-26.
- Yang, S.H. and Treiber, L.E. 1985. Chemical Stability of Polyacrylamide Under Simulated Field Conditions. Paper SPE 14232 presented at the SPE Annual Technical Conference and Exhibition, Las Vegas, Nevada, 22-25 September.
- You, Q., Zhao, F.L., Wang, Y.F., and Mu, L.N. 2007. Comparison of the Properties of Injected and Released Polyacrylamide in Polymer Flooding. *Journal of Beijing University of Chemical Technology*. **34**(4) 2007.414-417.
- Zhang, J. 1995. *The EOR Technology*. Beijing: Petroleum Industry Publishing Company of China.

## SI Metric Conversion Factors

cp x 1.0*	E-03	= Pa-s
ft x 3.048*	E-01	= m
in. x 2.54*	E+00	= cm
md x 9.869 233	E-04	= $\mu\text{m}^2$
psi x 6.894 757	E+00	= kPa